Problem of ''deformed'' superheavy nuclei

A. Sobiczewski,[1,2] I. Muntian,[1,2,3] and Z. Patyk[1,2]
[1]*Soltan Institute for Nuclear Studies, Hoża 69, PL-00-681 Warsaw, Poland*
[2]*Gesellschaft für Schwerionenforschung, D-64220 Darmstadt, Germany*
[3]*Institute for Nuclear Research, Kiev, Ukraine*
(Received 15 August 2000; published 12 February 2001)

The problem of experimental confirmation of deformed shapes of superheavy nuclei situated in the neighborhood of ^{270}Hs is discussed. Measurement of the energy E_{2+} of the lowest $2+$ state in even-even species of these nuclei is considered as a method for this confirmation. The energy is calculated in the cranking approximation for heavy and superheavy nuclei. Branching ratio p_{2+}/p_{0+} between α decay of a nucleus to this lowest $2+$ state and to the ground state $0+$ of its daughter is also calculated for these nuclei. The results indicate that a measurement of the energy E_{2+} for some superheavy nuclei by electron or α spectroscopy is a promising method for the confirmation of their deformed shapes.

DOI: 10.1103/PhysRevC.63.034306 PACS number(s): 21.10.Re, 21.60.Ev, 27.90.+b

I. INTRODUCTION

There is a fast progress in synthesis of superheavy nuclei (SHN) (cf. the reviews [1–3]). Two regions of these nuclei have been predicted theoretically: one around the spherical doubly magic nucleus ^{298}114 [4] and the other around deformed nuclei with $Z=108$–110 and $N=162$–164 (e.g., [5–10]). A detailed analysis of the ground-state energy of these nuclei and their single-particle spectra in a multidimensional deformation space [10] has led to ^{270}108 (^{270}Hs) as to a doubly magic deformed nucleus. For spherical SHN, a possibility of other proton closed shells at $Z=120$ [11] or $Z=126$ [12,11] has been also discussed.

The region of deformed SHN appears closer to experimentally investigated nuclei than that of spherical SHN. It was easier then to reach it, including also nuclei which are close to its center (^{270}Hs).

Large shell effects in deformed nuclei were not expected, because of less symmetry in their shapes and, consequently, of a more uniform distribution of energy levels in their spectra, as compared to spherical nuclei. Due to this, it was believed for a long time that only spherical SHN might exist (e.g., Refs. [13–15]).

Presently, although a number of SHN in the ''deformed'' region have been already observed, there is no experimental evidence for their deformed shapes. All indications are only of a theoretical nature. It is very important then to demonstrate experimentally that they are really deformed. This would show that a creation of a large energy gap of about 1.4 MeV [10] and, in consequence, a big increase of about 15 orders of magnitude or more [9,16,17] in fission half-lives are also possible in deformed heavy nuclei. It is because such huge shell effects are needed for the already observed existence of these nuclei. Without this strong shell structure, these nuclei would immediately decay.

The simplest way to confirm deformation of a nucleus is to observe a rotational band in its spectra. Presently, the heaviest nuclei for which such bands have been observed are ^{254,256}Fm [18]. Very recently, a rotational band has been also seen for ^{254}No [19,20] and ^{252}No [21]. There is, however, a small chance to observe such a band for superheavy nuclei, because cross sections to synthesize them are very low and the effectiveness of γ spectroscopy is relatively small. A more promising way is to see the first excited state $2+$ of an even-even nucleus in α decay or electron spectra. If the energy of such a state is found to be of about 40–50 keV, as is expected, the state cannot be of any other nature than rotational. An indication of this kind for deformation of the nucleus ^{256}Rf [22] was the observation of two close lines in the α-decay spectrum of ^{260}Sg [23].

The objective of this paper is to give help for such experiments by mainly calculating the equilibrium deformations, energies of the first $2+$ states, and the probabilities of α decay to these states for even-even superheavy nuclei in the deformed region. Some results of the study have been presented earlier [24].

This paper is organized as follows. Shell structure of superheavy nuclei is illustrated in Sec. II and the method of analysis is described in Sec. III. Section IV gives the results of the calculations and Sec. V presents a discussion of various effects. Finally, the conclusions drawn from the study are given in Sec. VI.

II. ILLUSTRATION OF THE SHELL STRUCTURE OF SHN

Figure 1 shows a contour map of the ground-state shell correction, $E_{\rm sh}$, calculated for a large region of nuclei with proton number $Z=82$–120 and neutron number $N=126$–190 [25]. One can see that the shell correction has three minima in the considered region. One (-14.3 MeV) is obtained for the experimentally well-known doubly magic spherical nucleus ^{208}Pb. The second (-7.2 MeV) appears at the nucleus ^{270}Hs, predicted to be doubly magic deformed nucleus [10]. The third (-7.2 MeV) is obtained for the nucleus ^{296}114, which is close to the nucleus ^{298}114 predicted to be doubly magic spherical nucleus [4]. It is interesting to note that the minima obtained for deformed (^{270}Hs) and spherical (^{296}114) nuclei are of comparable, here almost the same, depths.

Single-particle spectra calculated for these three doubly magic nuclei are shown in Figs. 2 and 3, for protons and

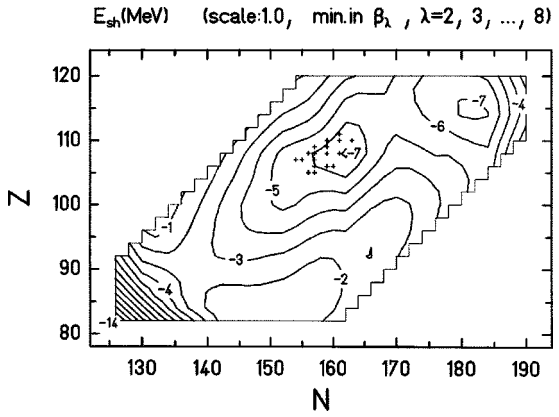

FIG. 1. Contour map of the ground-state shell correction energy E_{sh}. Crosses denote nuclei already synthesized [25].

neutrons, respectively. One can see in Fig. 2 large energy gaps at $Z=82$ (in the spectrum of ^{208}Pb), at $Z=108$ (in ^{270}Hs) and at $Z=114$ (in ^{298}114). For neutrons, besides a large energy gap at $N=162$ in the spectrum of ^{270}Hs, a smaller gap at $N=152$ is also seen. All this finds its reflection in the shell correction E_{sh}, shown in Fig. 1.

III. METHOD OF THE CALCULATIONS

A. Energy (mass) of a nucleus

The ground-state energy of a nucleus is calculated in a macroscopic-microscopic approach. The Yukawa-plus-exponential model [26] is taken for the macroscopic part of the energy and the Strutinski shell correction is used for the microscopic part. The Woods-Saxon single-particle potential, with the universal variant of its parameters found in Ref. [27], and also specified explicitly in Ref. [10] is taken as the basis for the shell correction.

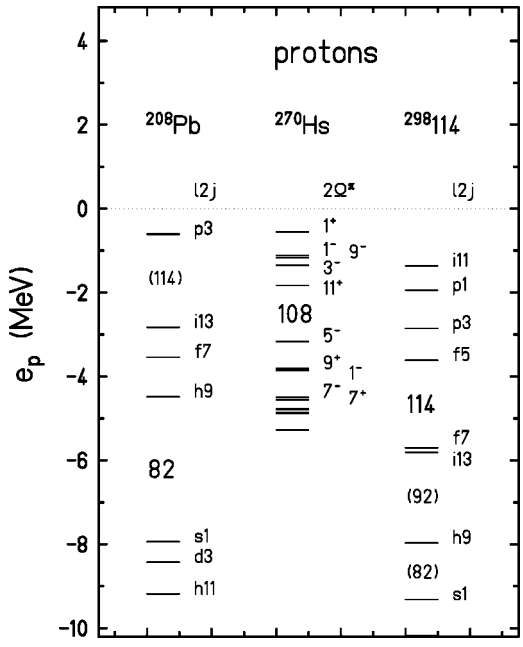

FIG. 2. Proton single-particle energy levels calculated for the doubly magic nuclei: ^{208}Pb, ^{270}Hs, and ^{298}114. Spectroscopic symbol for the orbital angular momentum l and total spin (multiplied by two) $2j$ are given at each level of the spherical nuclei ^{208}Pb and ^{298}114. Projection of spin on the symmetry axis of a nucleus (multiplied by two) 2Ω and parity π are shown at each level of the deformed nucleus ^{270}Hs.

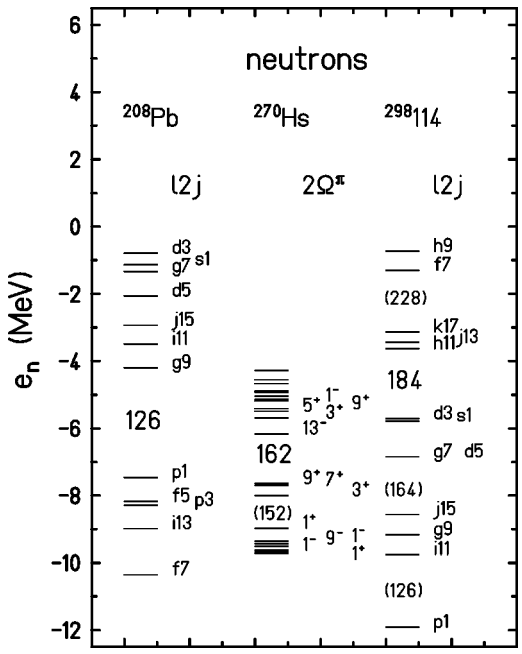

FIG. 3. Same as in Fig. 2, but for neutrons.

B. Equilibrium deformations

Equilibrium deformation of a nucleus is calculated by minimization of its energy in a multidimensional deformation space [28]. The seven-dimensional space $\{\beta_\lambda\}$, $\lambda=2,3,\ldots,8$, is taken. Here, β_λ are the usual deformation parameters, appearing in the expression for nuclear radius (in the intrinsic frame of reference) in terms of spherical harmonics (e.g., Ref. [28]). One can add here that, presently, besides the macroscopic-microscopic method (e.g., Refs. [25,29,30]), self-consistent approaches such as Hartree-Fock-Bogoliubov (e.g., Refs. [12,31]) and relativistic mean field (e.g., Ref. [32]) approximations are also used in the calculations of deformations of superheavy nuclei.

C. Moment of inertia

Moment of inertia of a nucleus is calculated in the cranking approximation [33]. It has been shown in a number of papers (e.g., Refs. [34–38]) that this approach allows for a good description of the ground-state moments of inertia of well deformed nuclei, especially of heavy ones [38]. In this paper, a multidimensional deformation space, particularly important for heaviest nuclei, is used for the calculation of moments of inertia. Also a final-depth (Woods-Saxon) single-particle potential is used instead of an infinite (modified oscillator) one, taken in older studies (e.g., Refs. [34–38]).

D. Probability of α decay to rotational states

Observation of α decay to the first rotational state $2+$, besides electron transitions, seems to be the most promising way to measure the energy of this state for heaviest nuclei. As cross section for synthesis of these nuclei is very small, it is very important to estimate, in a possibly realistic way, the probability of this decay, p_{2+}, to have an idea of a chance to observe it.

As a matter of fact, we are only interested in the branching ratio p_{2+}/p_{0+}, where p_{0+} is the probability of decay to the ground state $0+$ of a nucleus, as p_{0+}, itself (more exactly half-lives), has been already calculated for superheavy nuclei in a number of papers (e.g., Refs. [10,12,25,30,31]) and also measured for some of these nuclei. More generally, we can consider the ratio p_{I+}/p_{0+}. One should mention that the probabilities p_{I+} have been studied for already a long time (e.g., Ref. [39]).

The probability p_{I+} is usually considered as

$$p_{I+} = w_{I+} \cdot P_{I+}, \tag{1}$$

where w_{I+} is the reduced decay probability and P_{I+} is the probability to penetrate the potential-energy barrier by α particle with angular momentum I. Thus

$$p_{I+}/p_{0+} = (w_{I+}/w_{0+}) \cdot (P_{I+}/P_{0+}). \tag{2}$$

The penetration probability P_{I+} is calculated in the quasiclassical WKB approximation

$$P_{I+}(Z,N) = \exp\left\{ -\frac{2}{\hbar}\sqrt{2m_\alpha}\int_R^{r_T} [V(r)-E]^{1/2}\, dr \right\}, \tag{3}$$

where $V(r)$ is the potential energy as a function of the distance r between the centers of the α particle and the nucleus, and E is the decay energy of the parent nucleus to the state $I+$ of the considered nucleus (Z,N), i.e.,

$$E(Z,N) = Q_\alpha(Z+2,N+2) - E_{I+}(Z,N) \equiv Q_{\alpha p} - E_{I+}, \tag{4}$$

where E_{I+} is the rotational energy of the $I+$ state of a nucleus (Z,N) and $Q_{\alpha p}$ is the α-decay energy of the parent nucleus. The potential energy is

$$V(r) = \frac{2Ze^2}{r} + \frac{\hbar^2 I(I+1)}{2m_\alpha r^2}, \tag{5}$$

i.e., it is a superposition of the Coulomb and centrifugal energies. In Eq. (3), m_α is reduced mass of α particle, R is the value of r at the entrance point of α particle to the barrier, and r_T is the value of r at the exit point from the barrier. The entrance point is assumed to appear at $R = r_0 A^{1/3}$, i.e., at the radius of the nucleus, where A is its mass number and $r_0 = 1.4$ fm.

For low values of I, i.e., in the case of a low centrifugal barrier with respect to the Coulomb barrier, the integrand in Eq. (3) may be, in a good approximation, written as

$$\left[\left(\frac{2Ze^2}{r} - Q_{\alpha p}\right) + \left(\frac{\hbar^2 I(I+1)}{2m_\alpha r^2} + E_{I+}\right)\right]^{1/2} \simeq \left(\frac{2Ze^2}{r} - Q_{\alpha p}\right)^{1/2}\left[1 + \frac{1}{2}\left(\frac{\hbar^2 I(I+1)}{2m_\alpha r^2} + E_{I+}\right) \Big/ \left(\frac{2Ze^2}{r} - Q_{\alpha p}\right)\right], \tag{6}$$

because the second term in the first squared bracket is generally much smaller than the first term. This leads to the approximate equation

$$P_{I+}(Z,N) \simeq P_{0+}(Z,N)\cdot \exp\left\{ -\frac{\sqrt{2m_\alpha}}{\hbar}\int_R^{r_T}\left(\frac{\hbar^2 I(I+1)}{2m_\alpha r^2} + E_{I+}\right)\left(\frac{2Ze^2}{r} - Q_{\alpha p}\right)^{-1/2} dr \right\}$$
$$= P_{0+}(Z,N)\cdot \exp\left\{ -\frac{\sqrt{2m_\alpha}}{\hbar}\left[\left(\frac{\hbar^2 I(I+1)}{2m_\alpha}\frac{\sqrt{Q_{\alpha p}}}{Ze^2} + \frac{E_{I+}}{\sqrt{Q_{\alpha p}}}R\right)\left(\frac{B_C}{Q_{\alpha p}} - 1\right)^{1/2} + \frac{2Ze^2 E_{I+}}{Q_{\alpha p}^{3/2}}\arccos(Q_{\alpha p}/B_C)^{1/2}\right]\right\} \tag{7}$$

and, thus, to

$$P_{I+}/P_{0+} \simeq \exp\left\{ -\frac{\sqrt{2m_\alpha}}{\hbar}\left[\left(\frac{\hbar^2 I(I+1)}{2m_\alpha}\frac{\sqrt{Q_{\alpha p}}}{Ze^2} + \frac{E_{I+}}{\sqrt{Q_{\alpha p}}}R\right)\left(\frac{B_C}{Q_{\alpha p}} - 1\right)^{1/2} + \frac{2Ze^2 E_{I+}}{Q_{\alpha p}^{3/2}}\arccos(Q_{\alpha p}/B_C)^{1/2}\right]\right\}, \tag{8}$$

where P_{0+} is the probability of the penetration of α particle through the barrier with angular momentum $I=0$ and $B_C = 2Ze^2/R$ is height of the Coulomb barrier for α particle. A direct numerical check shows that the values of P_{I+}/P_{0+} obtained from Eqs. (8) and (3) are close to each other, especially for $I=2$. For example, the values P_{2+}/P_{0+} and P_{4+}/P_{0+} calculated by Eq. (8) for the nucleus $^{260}106$ (^{260}Sg) are 50.41 and 10.19, respectively, while cal-

culated with the use of the unapproximated WKB formula, Eq. (3), they are 51.01 and 10.90, respectively. Thus the value obtained by analytic formula of Eq. (8) deviates from that of Eq. (3) by only about 1% for P_{2+}/P_{0+} and by about 7% for P_{4+}/P_{0+}, for the nucleus ^{260}Sg.

The reason to derive the analytic formula of Eq. (8) is certainly not of the computational nature. The formula is derived to see explicitly the role of various quantities as $Q_{\alpha p}$, B_C, atomic number Z, or spin I in the ratio P_{I+}/P_{0+}. To calculate P_{I+} in our analysis, Eq. (3) has been used.

The ratio of reduced probabilities w_{I+}/w_{0+} is treated phenomenologically. Limiting ourselves to the lowest spin $I=2$, we find that the ratio may be well described by a two-parameter formula

$$w_{2+}/w_{0+}=10^{(aA+b)} \tag{9}$$

and, thus, the ratio of the total probabilities is

$$p_{2+}/p_{0+}=10^{(aA+b)}\cdot(P_{2+}/P_{0+}), \tag{10}$$

where A is the mass number of a nucleus.

Adjustment of the parameters a and b to experimental results for p_{2+}/p_{0+}, obtained for 26 nuclei [18] and shown in Table I, with P_{2+}/P_{0+} calculated with the use of Eq. (3), leads to the following values:

$$a=-0.02687, \qquad b=6.3608, \tag{11}$$

and reproduces the experimental values of p_{2+}/p_{0+} with rms deviations equal to 0.027.

E. Pairing interaction

The residual pairing interaction is treated in the BCS approximation. Its strength G_l, of the monopole and the isospin-dependent type, is taken in a rather usual form

$$A\cdot G_l=g_{0l}+g_{1l}I, \tag{12}$$

where A is the mass number of a nucleus, $I=(N-Z)/A$ is its relative neutron excess, and l stands for n (neutrons) or p (protons). To calculate potential energy of a nucleus and, consequently, its equilibrium deformation, mass, and quantities derived from them, we have taken the same values of the parameters g_{0l} and g_{1l} as those of the paper [10], where they have been fitted to odd-even mass differences of heavy nuclei. They are [10]

$$g_{0n}=19.86 \text{ MeV}, \quad g_{1n}=-21.4 \text{ MeV}, \quad \text{for } l=n \text{ (neutrons)}, \tag{13}$$

$$g_{0p}=17.98 \text{ MeV}, \quad g_{1p}=26.0 \text{ MeV}, \quad \text{for } l=p \text{ (protons)}.$$

However, as the moment of inertia of a nucleus is a sensitive function of the pairing strength (e.g., Ref. [35]), we have checked if the agreement between the calculated moments of inertia and experimental ones could be still improved by a small change of this strength. We have really found that a renormalization of the parameters g_{0l} and g_{1l}, given in Eq. (13), by a factor of 1.0529 (this is a slightly larger factor than that of 1.0485, used by us in earlier calculations [24]) improves the agreement significantly. Thus the moments of inertia of all nuclei studied in this paper are calculated with the strength parameters,

$$g_{0n}=20.91 \text{ MeV}, \quad g_{1n}=-22.5 \text{ MeV}, \quad \text{for } l=n \text{ (neutrons)}, \tag{14}$$

$$g_{0p}=18.93 \text{ MeV}, \quad g_{1p}=27.4 \text{ MeV}, \quad \text{for } l=p \text{ (protons)}.$$

A discussion of the sensitivity of the calculated moments of inertia to the pairing strength is presented in Sec. V B.

IV. RESULTS

A. Equilibrium deformations

As stated in Sec. III, all components β^0_λ, $\lambda=2,3,\ldots,8$ of the equilibrium deformation of the considered nuclei are studied. It is found, however, in accordance with Refs. [10,25,28] that the odd-multipolarity components β^0_λ, $\lambda=3,5,7$, are different from zero only for a very few of them. Due to this, only even-parity deformations β^0_λ, $\lambda=2,4,6,8$, are shown in our figures and tables. However, whenever results for nuclei with nonvanishing odd-parity deformations are presented, a remark on those deformations is done.

Contour maps of the deformations β^0_λ, $\lambda=2,4,6,8$, plotted as functions of proton Z and neutron N numbers are shown in Fig. 4. One can see that the main, quadrupole, component β^0_2 is the biggest one and it is positive in the whole considered region of deformed nuclei. It is large ($\beta^0_\lambda\approx 0.25$) and nearly constant in a big part of the region around the nucleus ^{254}No, and then outside of this part, it decreases rather fast with increasing N. The higher-multipolarity components are smaller and they change signs as one moves across the region. Still, even the deformations of so high multipolarity as $\lambda=6$ and 8 play a significant role in the properties of the nuclei, as will be illustrated in Sec. V A.

B. Rotational energies

1. The lowest state 2+

Before calculating the rotational energies E_{2+} for superheavy nuclei, we would like to test our calculations for nuclei, for which these energies have been measured. To this aim, the nuclei, which are good rotors, are taken. By good rotors, we mean the nuclei with $E_{4+}/E_{2+}\geqslant 3.00$. The results are given in Table I. To make the table more complete, we also included theoretical results for few nuclei, in which the experimental energy E_{2+} is not known yet but may be measured in a not too distant future.

The deformation energy $E_{\rm def}$, given in Table I, is defined as the difference between the energy of a nucleus at its

TABLE I. Ground-state equilibrium deformations β_λ^0, $\lambda=2,4,6,8$, deformation energy $E_{\rm def}$, moment of inertia J (multiplied by $2/\hbar^2$), and energy of the lowest $2+$ state, E_{2+}, calculated for nuclei specified in the first three columns.

Z	N	A	β_2^0	β_4^0	β_6^0	β_8^0	$E_{\rm def}$ MeV	$2J/\hbar^2$ MeV^{-1}	E_{2+} keV	$E_{2+}^{\rm exp}$ keV	$\frac{E_{4+}^{\rm exp}}{E_{2+}^{\rm exp}}$	$\frac{p_{2+}^{\rm exp}}{p_{0+}^{\rm exp}}$
88	138	226	0.151	0.087	0.017	−0.012	3.2	100.1	59.9	67.7	3.13	0.307
88	140	228	0.170	0.091	0.016	−0.013	3.9	107.8	55.6	63.8	3.21	0.284
88	142	230	0.188	0.093	0.011	−0.020	4.6	110.6	54.2	57.4	(3.25)	
88	144	232	0.202	0.087	−0.001	−0.023	5.2	115.4	52.0			
90	136	226	0.145	0.080	0.012	−0.011	3.5	97.0	61.8	72.2	3.14	0.475
90	138	228	0.176	0.108	0.032	−0.012	4.4	122.8	48.9	57.8	3.23	0.466
90	140	230	0.188	0.105	0.022	−0.015	5.4	122.7	48.9	53.2	3.27	0.398
90	142	232	0.199	0.100	0.012	−0.019	6.2	126.9	47.3	49.4	3.28	0.351
90	144	234	0.210	0.093	0.001	−0.022	6.8	128.0	46.9	49.6	3.29	0.265
90	146	236	0.221	0.085	−0.010	−0.024	7.1	129.2	46.5			
92	134	226	0.138	0.073	0.011	−0.006	2.9	90.3	66.5			
92	136	228	0.179	0.113	0.036	−0.008	4.3	134.0	44.8	59.		
92	138	230	0.189	0.113	0.029	−0.012	5.7	136.2	44.0	51.7	3.28	
92	140	232	0.199	0.109	0.020	−0.016	6.7	135.9	44.1	47.6	3.29	0.441
92	142	234	0.208	0.104	0.010	−0.019	7.6	139.1	43.1	43.5	3.30	0.409
92	144	236	0.217	0.097	0.000	−0.022	8.1	138.1	43.5	45.2	3.30	0.372
92	146	238	0.225	0.088	−0.011	−0.024	8.4	137.2	43.7	44.9	3.30	0.289
92	148	240	0.229	0.075	−0.018	−0.019	8.4	133.8	44.9	45.		0.241
92	150	242	0.232	0.056	−0.026	−0.008	8.1	125.0	48.0			
94	138	232	0.196	0.104	0.022	−0.013	6.3	127.9	46.9			
94	140	234	0.207	0.102	0.012	−0.016	7.5	131.1	45.8			
94	142	236	0.215	0.095	0.002	−0.019	8.4	135.3	44.4	44.6	3.30	0.408
94	144	238	0.223	0.091	−0.006	−0.022	9.1	137.9	43.5	44.1	3.31	0.338
94	146	240	0.231	0.083	−0.015	−0.023	9.5	140.0	42.9	42.8	3.31	0.309
94	148	242	0.233	0.070	−0.022	−0.017	9.5	136.1	44.1	44.5	3.31	0.217
94	150	244	0.235	0.054	−0.029	−0.007	9.3	129.0	46.5	46.0		0.220
94	152	246	0.239	0.037	−0.036	0.001	8.9	127.1	47.2			
94	154	248	0.239	0.026	−0.037	0.006	8.1	122.8	48.9			
96	144	240	0.228	0.081	−0.014	−0.018	9.8	135.8	44.2	38.		0.33
96	146	242	0.235	0.074	−0.022	−0.019	10.3	140.0	42.9	42.1	3.28	0.260
96	148	244	0.237	0.064	−0.027	−0.014	10.5	138.1	43.4	43.0	3.31	0.222
96	150	246	0.240	0.049	−0.033	−0.006	10.3	133.0	45.1	42.9	3.31	0.179
96	152	248	0.242	0.035	−0.039	0.001	10.0	132.6	45.3	43.4	3.31	0.186
96	154	250	0.242	0.024	−0.040	0.006	9.2	128.0	46.9	43.		0.207
98	146	244	0.239	0.065	−0.029	−0.015	10.8	138.0	43.5	40.		0.25
98	148	246	0.241	0.055	−0.035	−0.011	11.1	137.3	43.7			
98	150	248	0.243	0.042	−0.040	−0.004	11.1	134.8	44.5	41.5	3.32	0.179
98	152	250	0.246	0.029	−0.045	0.002	10.8	137.7	43.6	42.7	3.32	0.167
98	154	252	0.246	0.020	−0.045	0.007	10.1	133.2	45.1	45.7	3.32	
98	156	254	0.244	0.008	−0.044	0.013	9.1	124.6	48.2			
98	158	256	0.240	−0.005	−0.041	0.017	8.0	118.2	50.8			
100	150	250	0.248	0.033	−0.046	−0.002	11.5	136.8	43.9			
100	152	252	0.250	0.022	−0.051	0.004	11.4	143.0	42.0			
100	154	254	0.249	0.013	−0.051	0.009	10.7	138.2	43.4	45.0	3.32	
100	156	256	0.247	0.001	−0.049	0.015	9.7	129.3	46.4	48.2	3.31	
100	158	258	0.243	−0.012	−0.044	0.019	8.7	122.6	48.9			
100	160	260	0.235	−0.026	−0.034	0.019	7.8	119.3	50.3			

spherical and equilibrium shapes, i.e.,

$$E_{\rm def}\equiv E(0)-E(\beta_\lambda^0). \tag{15}$$

Thus it is the gain in energy of a nucleus due to its deformation. This quantity tells us how well the deformation of a nucleus is established or, in other words, how small are the zero-point fluctuations of its shape with respect to its equilibrium shape. One can say, in practice, that nuclei with $E_{\rm def}\gtrsim 2$ MeV are well deformed (e.g., Ref. [36]). It is seen in Table I that, according to the calculations, all nuclei considered in it are well deformed.

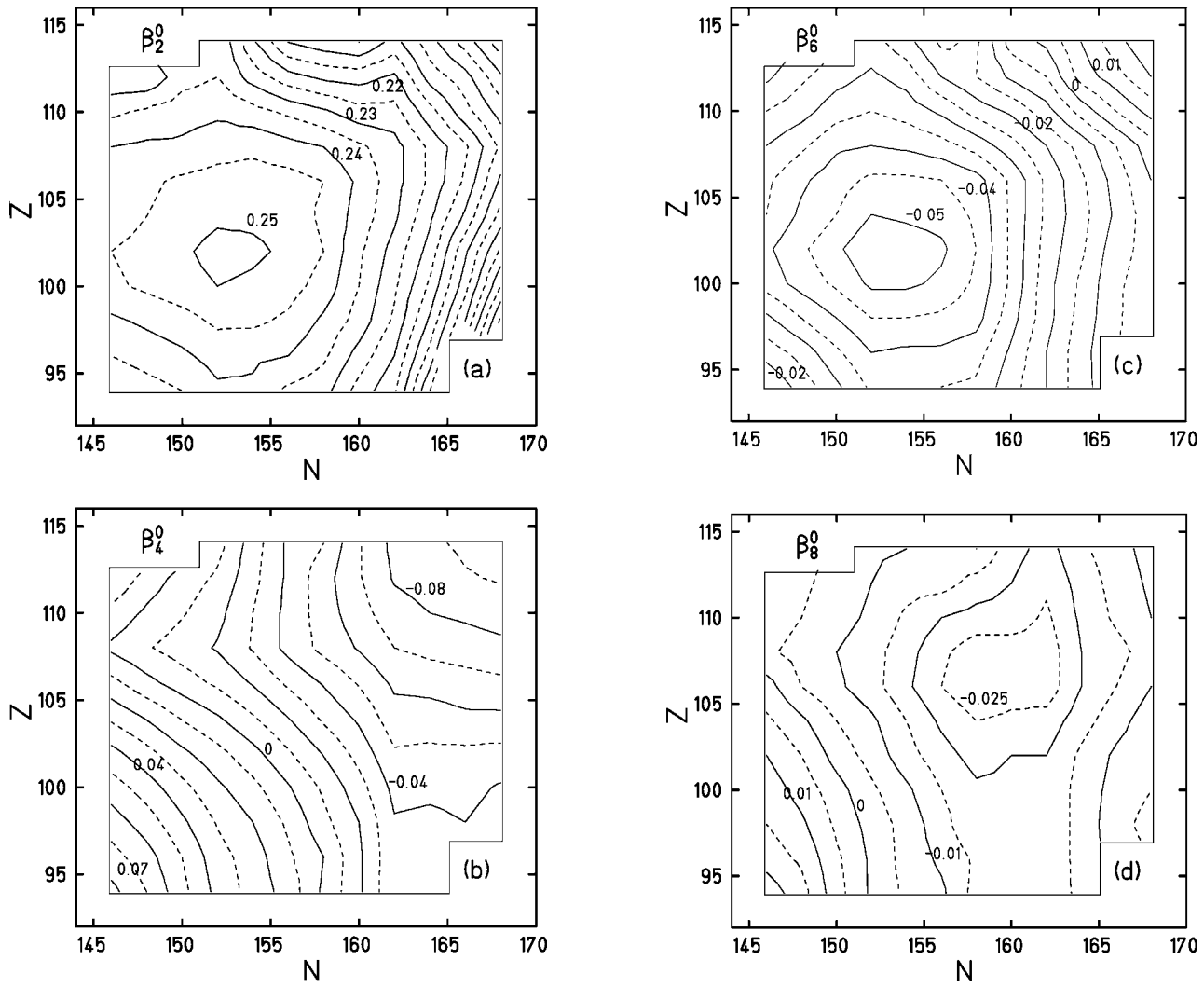

FIG. 4. Contour maps of the equilibrium deformations β_λ^0, $\lambda=2,4,6,8$, plotted as functions of proton Z and neutron N numbers in the region: $Z=94$–114, $N=146$–168. Numbers at the contour lines give the values of the deformations.

The rotational energy in the $I+$ state, E_{I+}, is connected with the moment of inertia J by the usual formula

$$E_{I+}=(\hbar^2/2J)I(I+1). \tag{16}$$

For the ideal rotor, i.e., with J independent of I, which we assume here, the quantities J and E_{I+} are equivalent and the specification of both J and E_{2+} in Table I is done only for the reason of convenience, as both quantities are used in various studies. The ratio $E_{4+}^{\rm exp}/E_{2+}^{\rm exp}$, specified in the last but one column, tells us how good rotor is a given nucleus. The last column gives experimental values for the branching ratio p_{2+}/p_{0+}. All experimental values given in Table I are taken from Ref. [18].

One can see in Table I that 27 experimental values of E_{2+} (those with all three digits given) are reproduced very well (rms=4.1 keV). They are particularly well reproduced for 15 especially good rotors (with $E_{4+}/E_{2+}\geqslant 3.30$); the value of the rms deviations for them is 1.4 keV.

For complete knowledge on the calculated deformations of nuclei presented in Table I, one should add that only three of them, ^{226}Ra, ^{226}Th, and ^{226}U, have the odd-multipolarity deformations β_λ^0, $\lambda=3,5,7$, different from zero. The values of the deformations for these three nuclei are $(\beta_3^0,\beta_5^0,\beta_7^0)=(0.079,0.027,0.009)$, $(0.102,0.037,0.010)$, and $(0.105, 0.037, 0.011)$, respectively.

In a graphic form, the relation between theoretical and experimental values of E_{2+} is illustrated in Fig. 5. One can see that for nuclei heavier than ^{234}U, which are especially good rotors, the agreement between theory and experiment is really very good.

Contour map of the energy E_{2+} calculated for a wide region of nuclei with $Z=94$–114 and $N=146$–168 is shown in Fig. 6 [24]. One can see that two minima of E_{2+} are obtained for the considered nuclei. One of them (41.6 keV) is obtained for the nucleus ^{254}No and the other (40.2 keV) for ^{270}Hs. (One can note that the calculated value 41.6 keV for ^{254}No is close to the value 44 keV, deduced from recent measurements [19,20].) The two minima of E_{2+} make the view of the map of this quantity rather unusual, specific for the superheavy region. Usually, such a map has only one

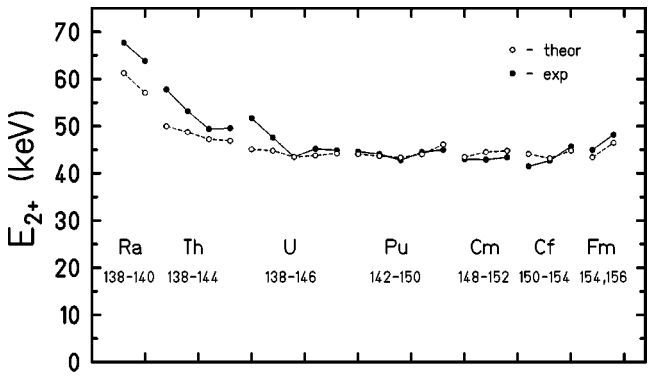

FIG. 5. Comparison between theoretical and experimental values of the energy E_{2+} of the first rotational state $2+$. For each element, values of neutron number N of the considered isotopes are specified below the symbol of the element.

minimum for each region of deformed nuclei, and is similar to the map of the main (quadrupole) component of the equilibrium deformation, β_2^0, of the nuclei. This similarity is rather natural due to the strong dependence of the moment of inertia J on β_2^0. Both these usual properties of the E_{2+} map can be seen, e.g., for the regions of light-barium and also of rare-earth nuclei, studied in Ref. [36].

The dissimilarity of the maps of E_{2+} and of β_2^0 for superheavy nuclei, which can be seen by comparing Figs. 4 and 6, has two main reasons. One is that deformations of higher multipolarities are more important in very heavy nuclei [28], like considered in this paper, than in lighter deformed nuclei. The other, more important reason is the exceptional shell structure of the nuclei studied, or more particularly, the appearance of strong *deformed* shells (closed at $N=162$ and $Z=108$) and a weaker shell (closed at $N=152$) in this structure (e.g., Ref. [10]) not observed in lighter deformed nuclei. These two reasons are connected, one with the other, as deformations of higher multipolarities contribute to the creation of these shells and thus to creation of these minima of E_{2+}.

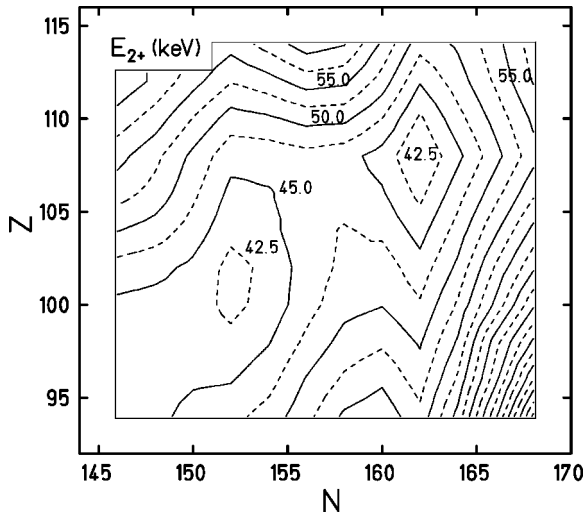

FIG. 6. Contour map of calculated energy E_{2+} of the first rotational state $2+$.

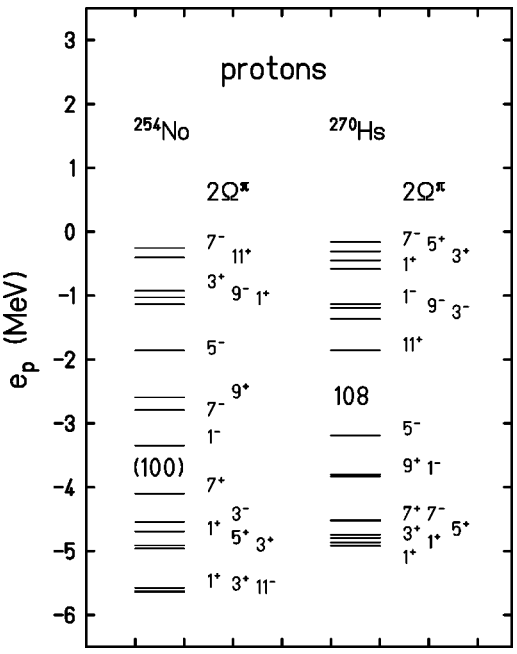

FIG. 7. Proton single-particle energy levels e_p calculated for the nuclei: ^{254}No and ^{270}Hs. Projection of spin on the symmetry axis of a nucleus (multiplied by two) 2Ω and parity π are shown at each level.

The role of deformations of various multipolarities in the moment of inertia and thus in E_{2+} is discussed in Sec. V A.

It is interesting to see the single-particle structure of the nuclei ^{254}No and ^{270}Hs, in which the minima of E_{2+} have been obtained in Fig. 6. The structure is shown in Figs. 7 and 8 for protons and neutrons, respectively. One can see rather large energy gaps at $N=162$ (about 1.5 MeV) and $Z=108$ (about 1.3 MeV) for the nucleus ^{270}Hs, and a slightly smaller

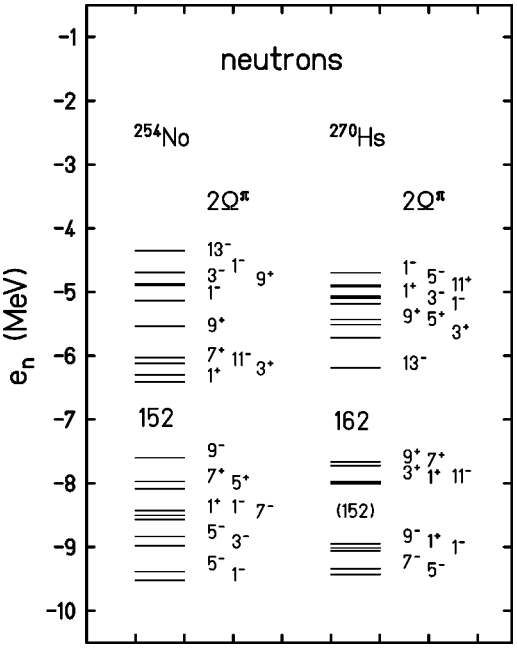

FIG. 8. Same as in Fig. 7, but for neutrons.

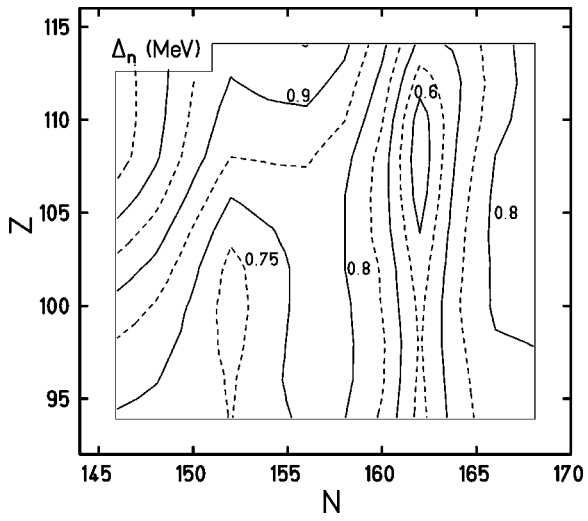

FIG. 9. Same as in Fig. 6, but for the neutron pairing-energy gap parameter Δ_n.

gap at $N=152$ (about 1.2 MeV) in the nucleus ^{254}No. Only a rather small gap (about 0.6 MeV) appears in the latter nucleus at $Z=102$, even smaller than that at $Z=100$ (about 0.8 MeV).

The energy gaps (closed shells or subshells) influence the values of moments of inertia and thus of E_{2+} of nuclei by weakening the pairing correlations, to which moments of inertia are very sensitive (e.g., Ref. [35]). To illustrate this, we plot in Fig. 9 the map of the pairing energy gap, Δ_n, for neutrons. One can see that the shell closures at $N=152$ and 162 result in small values (local minima) of Δ_n, which lead to large values of the moment of inertia and, this way, to small values of E_{2+}.

To see more clearly, than in Fig. 6, the dependence of E_{2+} on neutron number N around the shell closures at $N=152$ and 162, this energy is plotted in Fig. 10 as a function of N for $Z=102-112$. One can see clear effects of the deformed shells at $N=152$ and 162. Numerical values of E_{2+}, as well as those of equilibrium deformations, deformation energies, moments of inertia, and transition energies from $4+$ to $2+$ states (to be possibly measured by electron spectroscopy), E_{42}, for nuclei with $Z=102-112$, are given in Table II.

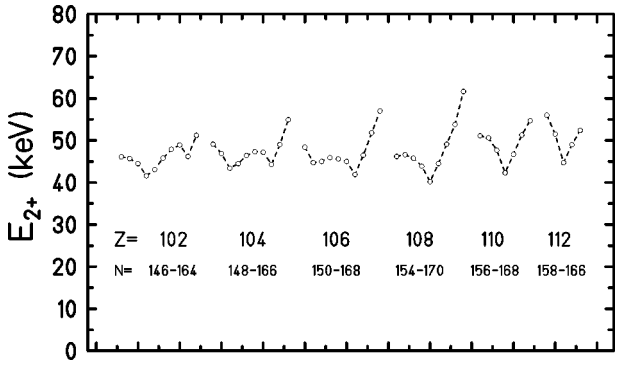

FIG. 10. Dependence of the energy E_{2+} on neutron number N, calculated for elements with proton number $Z=102-112$. For each element, values of considered N are specified below the value of Z.

2. Higher states

As the objective of this paper is to describe only the energy of the lowest rotational state $2+$ in the heaviest even-even nuclei, we do not study higher states. It is still worth noting that the calculated ground-state moments of inertia well describe the rotational energies of also higher states, up to spin 8, 10, and even 14. In particular, all transition energies up to spin 8 in all 15 good rotors ($E^{\rm exp}_{4+}/E^{\rm exp}_{2+} \geqslant 3.30$), shown in Table I, are described by our moments of inertia with the accuracy better than 10 keV. In the recently studied nucleus ^{254}No [19,20], all measured transition energies up to that of $14+ \rightarrow 12+$ are reproduced with a better accuracy than 8 keV (i.e., the absolute value of the discrepancy between calculated and measured values does not exceed 8 keV).

C. Branching ratio p_{2+}/p_{0+}

The branching ratio p_{2+}/p_{0+} calculated for the nuclei with $Z=88-98$, i.e., for these nuclei in which experimental values of it are known, is shown in Fig. 11. It is obtained with the use of Eq. (10) with the parameters of Eq. (11). One can see that the calculated values reproduce the experimental data quite well. In particular, a rather strong isotopic dependence of p_{2+}/p_{0+} is well reproduced.

The ratio p_{2+}/p_{0+} calculated for heavier nuclei with $Z=102-112$ is shown in Fig. 12. One can see that a rather strong dependence of it on the neutron number also appears for these nuclei. It has important implication for planning experiments for the observation of the $2+$ state. In particular, to have a reasonable chance to observe this state in a heavy element, one should take for this as light an isotope of it as possible. Numerical values of p_{2+}/p_{0+} are given in Table II. The α-decay energies of the parent nuclei to given ones are also presented in the table.

To see the role of the phenomenological term $10^{(aA+b)}$ in the branching ratios presented in Figs. 11 and 12 and in Table II, let us specify a few values of it. For the lightest nucleus considered in Fig. 11, ^{226}Ra, it is equal to 1.94; and for the heaviest one, ^{250}Cf, its value is 0.440. Thus it decreases by a factor of 4.4 between these two nuclei. Between the lightest, ^{248}No, and the heaviest, ^{278}112, nuclei considered in Fig. 12 and Table II, it decreases by a factor of 6.4. This way, this term decides the rather fast decrease of the branching ratio with the increasing mass number A.

V. DISCUSSION OF VARIOUS EFFECTS

A. Role of deformations of various multipolarities in the moment of inertia

To illustrate the importance of using a multidimensional deformation space for the calculations of the moments of inertia of nuclei, let us show the dependence of them on the dimension of the space used. As in earlier discussion, instead of the moment of inertia J itself, we use the equivalent to it and directly measurable quantity E_{2+}. For the illustration, we take the nuclei, for which E_{2+} are smallest, i.e., the nuclei ^{254}No and ^{270}Hs.

TABLE II. Ground-state equlibrium deformations β_λ^0, $\lambda=2,4,6,8$, deformation energy $E_{\rm def}$, moment of inertia J (multiplied by $2/\hbar^2$), energy of the lowest $2+$ state, E_{2+}, energy of the transition $4+ \rightarrow 2+$, E_{42}, α-decay energy of the parent nucleus $Q_{\alpha p}$, and branching ratio p_{2+}/p_{0+}, calculated for nuclei specified in the first three columns.

Z	N	A	β_2^0	β_4^0	β_6^0	β_8^0	$E_{\rm def}$ MeV	$2J/\hbar^2$ MeV^{-1}	E_{2+} keV	E_{42} keV	$Q_{\alpha\rm p}$ MeV	$\frac{p_{2+}}{p_{0+}}$ %
102	146	248	0.245	0.043	−0.039	−0.010	10.6	130.0	46.1	108	9.85	24.2
102	148	250	0.247	0.033	−0.044	−0.005	11.2	131.4	45.7	107	9.43	20.9
102	150	252	0.249	0.022	−0.049	0.002	11.5	134.8	44.5	104	9.10	18.3
102	152	254	0.252	0.013	−0.054	0.007	11.5	144.1	41.6	97	9.20	16.6
102	154	256	0.251	0.003	−0.053	0.013	10.9	139.2	43.1	101	8.84	14.2
102	156	258	0.249	−0.009	−0.051	0.018	10.0	131.0	45.8	107	8.26	11.8
102	158	260	0.245	−0.021	−0.045	0.022	9.1	125.4	47.9	112	7.70	9.7
102	160	262	0.236	−0.034	−0.034	0.020	8.3	122.6	48.9	114	7.15	8.0
102	162	264	0.228	−0.049	−0.023	0.020	7.5	129.8	46.2	108	7.64	7.7
102	164	266	0.218	−0.048	−0.016	0.014	6.0	117.2	51.2	119	7.40	6.3
104	148	252	0.245	0.019	−0.041	−0.001	10.6	122.2	49.1	115	10.19	18.9
104	150	254	0.247	0.009	−0.045	0.005	11.1	127.9	46.9	109	9.90	16.6
104	152	256	0.249	0.001	−0.050	0.009	11.3	138.2	43.4	101	9.96	15.1
104	154	258	0.249	−0.009	−0.049	0.015	10.8	134.8	44.5	104	9.60	13.0
104	156	260	0.248	−0.020	−0.048	0.021	10.1	129.3	46.4	108	9.06	11.0
104	158	262	0.244	−0.032	−0.044	0.025	9.3	126.8	47.3	110	8.54	9.3
104	160	264	0.238	−0.042	−0.034	0.024	8.6	127.1	47.2	110	8.05	7.9
104	162	266	0.231	−0.055	−0.024	0.023	7.9	135.5	44.3	103	8.66	7.5
104	164	268	0.221	−0.055	−0.017	0.017	6.4	122.4	49.0	114	8.46	6.3
104	166	270	0.209	−0.058	−0.009	0.012	4.9	109.2	54.9	128	8.11	5.1
106	150	256	0.246	−0.005	−0.043	0.009	10.5	123.9	48.4	113	10.97	15.4
106	152	258	0.247	−0.012	−0.046	0.013	10.8	134.1	44.7	104	11.02	13.9
106	154	260	0.247	−0.021	−0.046	0.019	10.5	133.4	45.0	105	10.69	12.1
106	156	262	0.247	−0.032	−0.045	0.025	9.9	130.8	45.9	107	10.20	10.4
106	158	264	0.245	−0.041	−0.042	0.029	9.3	131.5	45.6	106	9.65	8.9
106	160	266	0.239	−0.051	−0.034	0.027	8.7	133.4	45.0	105	9.13	7.7
106	162	268	0.232	−0.062	−0.024	0.028	8.0	143.1	41.9	98	9.79	7.2
106	164	270	0.224	−0.064	−0.016	0.020	6.5	129.0	46.5	109	9.58	6.1
106	166	272	0.214	−0.066	−0.008	0.015	5.0	115.9	51.8	121	9.22	5.1
106	168	274	0.199	−0.067	−0.001	0.011	3.7	105.2	57.0	133	8.77	4.2
108	154	262	0.244	−0.031	−0.039	0.018	9.6	129.9	46.2	108	12.17	11.3
108	156	264	0.242	−0.043	−0.037	0.024	9.2	128.7	46.6	109	11.76	9.8
108	158	266	0.240	−0.053	−0.033	0.028	8.7	131.1	45.8	107	11.24	8.5
108	160	268	0.236	−0.061	−0.027	0.028	8.2	136.6	43.9	102	10.80	7.5
108	162	270	0.232	−0.070	−0.020	0.028	7.8	149.4	40.2	94	11.39	6.9
108	164	272	0.224	−0.073	−0.013	0.020	6.3	134.8	44.5	104	11.03	5.9
108	166	274	0.216	−0.075	−0.005	0.017	4.8	122.2	49.1	115	10.52	4.9
108	168	276	0.204	−0.077	0.003	0.012	3.5	111.6	53.8	125	9.84	4.1
108	170	278	0.177	−0.070	0.007	0.007	2.4	97.4	61.6	144	8.86	3.2
110	156	266	0.234	−0.043	−0.029	0.020	7.5	117.5	51.1	119	12.59	8.8
110	158	268	0.231	−0.055	−0.023	0.022	7.1	118.5	50.6	118	12.07	7.6
110	160	270	0.227	−0.066	−0.019	0.022	6.7	125.8	47.7	111	11.67	6.7
110	162	272	0.227	−0.076	−0.012	0.026	6.4	141.8	42.3	99	12.13	6.2
110	164	274	0.217	−0.080	−0.003	0.019	5.2	128.5	46.7	109	11.83	5.3
110	166	276	0.207	−0.082	0.005	0.014	3.9	117.0	51.3	120	11.36	4.5
110	168	278	0.198	−0.085	0.012	0.010	2.8	109.6	54.7	128	10.65	3.8
112	158	270	0.219	−0.056	−0.015	0.017	5.3	107.1	56.0	131	12.76	6.7
112	160	272	0.218	−0.069	−0.009	0.020	5.1	116.6	51.5	120	12.41	6.0
112	162	274	0.221	−0.081	−0.005	0.024	4.9	134.3	44.7	104	12.75	5.5
112	164	276	0.208	−0.084	0.007	0.018	3.9	122.5	49.0	114	12.54	4.8
112	166	278	0.202	−0.089	0.013	0.013	2.8	114.6	52.4	122	12.13	4.1

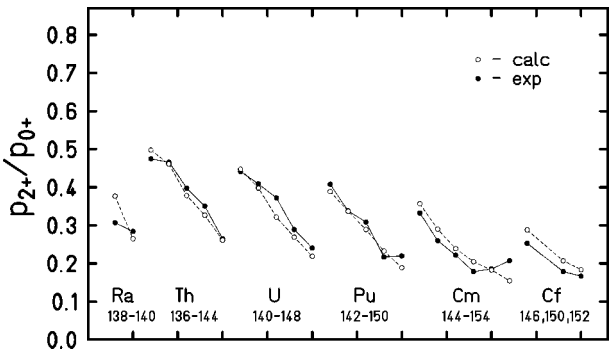

FIG. 11. Comparison between calculated and experimental values of the branching ratio p_{2+}/p_{0+} for nuclei of the elements Ra–Cf, with neutron numbers N specified below the symbol of each element.

Figure 13 shows the dependence of E_{2+} on the maximal multipolarity $\lambda_{\max}$ included in the used deformation space $\{\beta_\lambda\}$, $\lambda=2,4,\ldots,\lambda_{\max}$, for the nucleus ^{254}No. One can see that the energy E_{2+} is rather large (50.6 keV) at the equilibrium shape of this nucleus, when only one-dimensional space ($\lambda_{\max}=2$) is used. It is only slightly decreased (to 50.1 keV, i.e., by about 1%) when the second dimension ($\lambda=4$) is included, but is essentially lowered (to 41.7 keV, i.e., by about 17%) when the third dimension ($\lambda=6$) is added. The inclusion of the fourth dimension ($\lambda=8$) lowers E_{2+} to 41.6 keV only very little. Thus the analysis of E_{2+} in the four-dimensional space gives $E_{2+}=41.6$ keV, instead of $E_{2+}=50.6$ keV obtained in a one-dimensional space. Figure 14 shows similar dependence of E_{2+} for ^{270}Hs. One can see here that the inclusion of the deformation β_4 decreases E_{2+} from 59.9 keV to 44.2 keV; i.e., by about 26%, the inclusion of β_6 further lowers it to 42.7 keV and the addition of β_8 decreases it to 40.2 keV. Thus, for the nucleus ^{270}Hs, the inclusion of β_4 is very important, but addition of very high multipolarity as $\lambda=8$ is also significant.

Figures 13 and 14 show the importance of using a multidimensional deformation space in the analysis of nuclear moments of inertia. The significance of a given multipolarity is, however, the individual property of a nucleus. For some nuclei, certain multipolarities are important; for other ones, other multipolarities are of the largest significance.

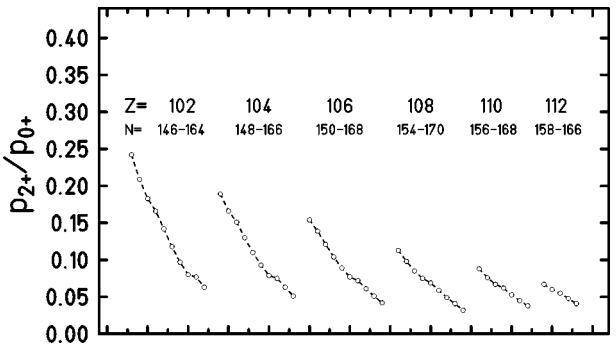

FIG. 12. Same as in Fig. 10, but for the branching ratio p_{2+}/p_{0+}.

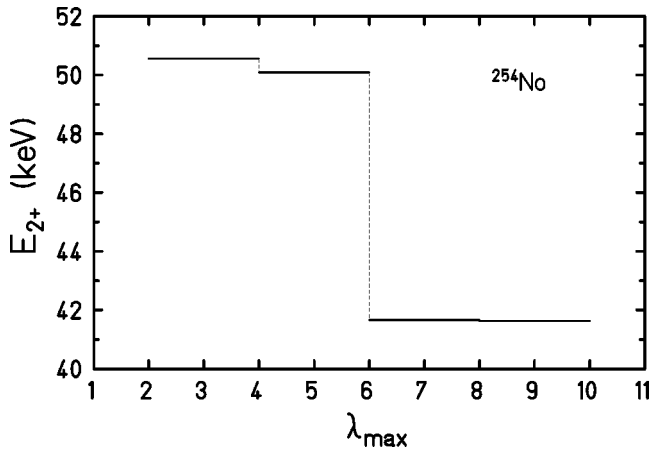

FIG. 13. Dependence of the energy E_{2+} on the maximal multipolarity $\lambda_{\max}$ included in the used deformation space $\{\beta_\lambda\}$, $\lambda=2,4,\ldots,\lambda_{\max}$, for the nucleus ^{254}No.

Concerning the highest λ, which should be taken into account, the analysis of the binding energy of heavy nuclei [10] has shown that the multipolarities $\lambda\geqslant 10$ may already be disregarded.

B. Sensitivity to strength of pairing interaction

To discuss the sensitivity of our results for the energy E_{2+} to the pairing interaction strength G_l, Eq. (12), we change this quantity in a wide region: $(0.80–1.20)G_l$ and look at the resulting changes in six important quantities: proton and neutron pairing-energy gap parameters, Δ_p and Δ_n; proton and neutron contribution to the moment of inertia, J_p and J_n; and total moment of inertia J and the rotational energy E_{2+}. For the illustration, we choose the nucleus ^{260}Sg, which is one of candidates for the measurement of E_{2+}.

Figure 15 shows the dependence of Δ_p and Δ_n on c, where c is a multiplication factor of G. Thus $c=1$ corresponds to not changed G given by Eq. (13), i.e., to G adjusted to odd-even mass differences of heavy nuclei [10] and $c=1.0529$ corresponds to G given by Eq. (14), with

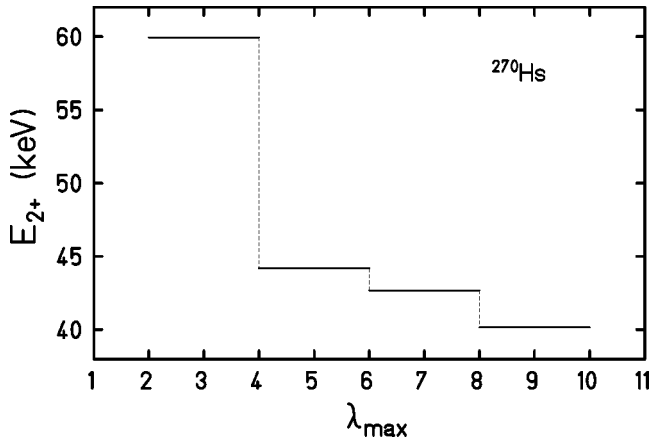

FIG. 14. Same as in Fig. 13, but for the nucleus ^{270}Hs.

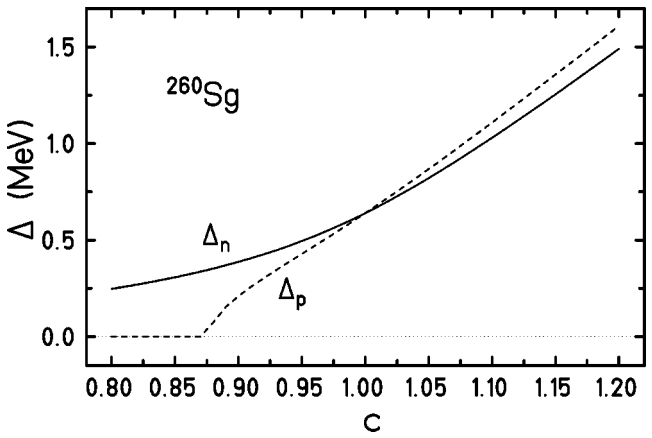

FIG. 15. Dependences of the proton and neutron pairing-energy gap parameters Δ_p and Δ_n, respectively, on the pairing strength factor c, calculated for the nucleus ^{260}Sg.

which moments of inertia of all nuclei studied in this paper are calculated. One can see in Fig. 15 that both values, $c=1$ (with which equilibrium deformations, masses, and quantities connected with them are calculated) and $c=1.0529$ (with which moments of inertia are calculated) are far from the critical value $c_{\rm cr}$ at which the BCS approximation collapses. Thus, with the pairing strength used by us, this approximation is good. It is seen in Fig. 15 that $c_{\rm cr}=0.87$ for protons and $c_{\rm cr}<0.80$ for neutrons, for the studied nucleus ^{260}Sg. One can also see that the increase of c by 5% from $c=1$ changes Δ_p from 0.64 MeV to 0.89 MeV, i.e., by about 36% and Δ_n from 0.63 MeV to 0.82 MeV, i.e., by about 29%. Figure 16 illustrates the dependence of proton, J_p, and neutron, J_n, contributions to the total moments of inertia J, as well as of J itself. The increase of c by 5% from $c=1$ decreases $2J_p/\hbar^2$ from 59.4 MeV^{-1} to 52.1 MeV^{-1}, i.e., by about 12%, $2J_n/\hbar^2$ from 95.9 MeV^{-1} to 82.5 MeV^{-1}, i.e., by about 14% and $2J/\hbar^2$ from 155.3 MeV^{-1} to 134.6 MeV^{-1}, i.e., by about 13%. Finally, Fig. 17 shows the dependence of the energy E_{2+} on c. One can see that the increase of c by 5% from $c=1$ results in the

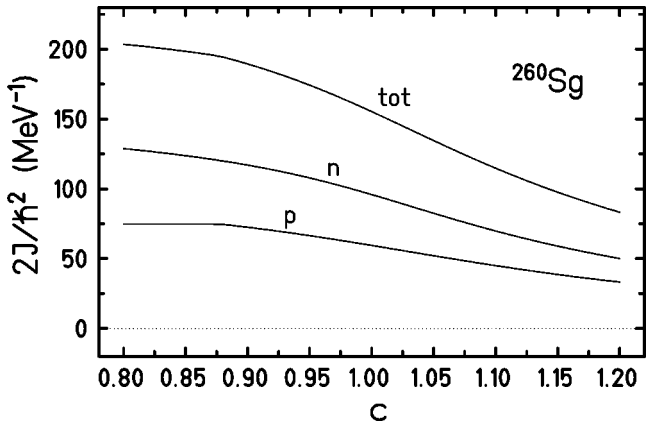

FIG. 16. Same as in Fig. 15, but for the total (tot) moment of inertia J and the proton (p), J_p, and neutron (n), J_n, contributions to it, all multiplied by a factor of $2/\hbar^2$.

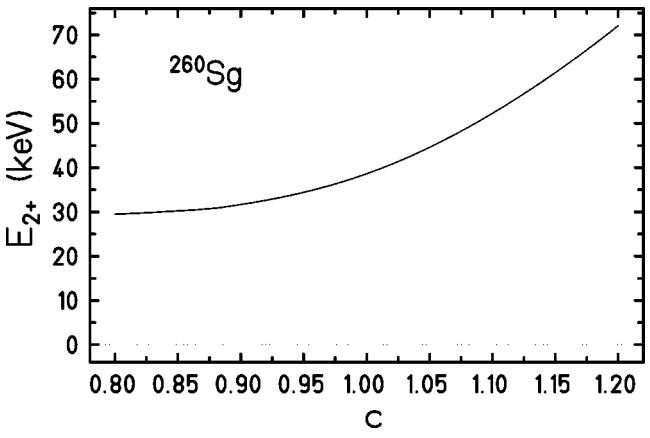

FIG. 17. Same as in Fig. 15, but for the energy E_{2+} of the lowest rotational state $2+$.

increase of E_{2+} from 38.6 keV to 44.6 keV, i.e., by about 16%.

VI. CONCLUSIONS

The following conclusions may be drawn from our study:

(1) A very good description of energy of the lowest rotational states $2+$ of heaviest even-even nuclei is obtained within the cranking approximation. In particular, the energies of 15 nuclei of the elements from uranium to fermium, which are very good rotors ($E_{4+}/E_{2+}\geqslant 3.30$), are described with the average accuracy (rms) of 1.4 keV.

(2) Higher states are also quite well described. For example, all transition energies, including the one of $14+\rightarrow 12+$, measured recently in the rotational band of ^{254}No [19,20] agree with the calculated ones with a better accuracy than 8 keV.

(3) Sufficiently large deformation space is needed for a proper description of rotational energies (moments of inertia) of heaviest nuclei. For example, inclusion of the deformation of so high multipolarity as $\lambda=6$ changes the moment of inertia of the nucleus ^{254}No by so much as 17%.

(4) Shell structure of deformed superheavy nuclei is clearly reflected in their rotational properties. In particular, the rotational energy E_{2+} is lowest (i.e., moment of inertia is highest) for nuclei with closed deformed shells (see Fig. 6). The mechanism is that pairing correlations are weakened at closed shells and, as a result, moment of inertia is increased (i.e., moving in the direction to its rigid body limit), so the rotational energy is decreased.

(5) Branching ratio p_{2+}/p_{0+} between α decay of a nucleus to the first rotational state $2+$ and to the ground state $0+$ of its daughter has a strong isotopic dependence. The dependence mainly comes from the behavior of the ratio of reduced probabilities w_{2+}/w_{0+}. To have the ratio p_{2+}/p_{0+} sufficiently large, one should take in experiment as light isotope of a given element as possible.

ACKNOWLEDGMENTS

The authors would like to thank S. Hofmann, T.L. Khoo, M. Leino, and G. Münzenberg for discussions on the possi-

bilities of measuring the rotational energies of heaviest nuclei and on the experimental studies presently being done or prepared. They are also grateful to P. Armbruster, P. Butler, J. Gerl, W. Nörenberg, J. Styczeń, and H.J. Wollersheim for helpful comments. Support by the Polish State Committee for Scientific Research (KBN), Grant No. 2 P03B 117 15, and by the Bogoliubov-Infeld Programme is gratefully acknowledged.

[1] S. Hofmann, Rep. Prog. Phys. **61**, 639 (1998); Acta Phys. Pol. B **30**, 621 (1999).
[2] Yu.Ts. Oganessian, in *Heavy Elements and Related New Phenomena*, edited by W. Greiner and R.K. Gupta (World Scientific, Singapore, 1999), Vol. 1, Chap. 2.
[3] S. Hofmann and G. Münzenberg, Rev. Mod. Phys. **72**, 733 (2000).
[4] A. Sobiczewski, F.A. Gareev, and B.N. Kalinkin, Phys. Lett. **22**, 500 (1966); H. Meldner, Ark. Fys. **36**, 593 (1967).
[5] S. Ćwiok, V.V. Pashkevich, J. Dudek, and W. Nazarewicz, Nucl. Phys. **A410**, 254 (1983).
[6] P. Möller, G.A. Leander, and J.R. Nix, Z. Phys. A **323**, 41 (1986).
[7] K. Böning, Z. Patyk, A. Sobiczewski, and S. Ćwiok, Z. Phys. A **325**, 479 (1986).
[8] A. Sobiczewski, Z. Patyk, and S. Ćwiok, Phys. Lett. B **186**, 6 (1987).
[9] Z. Patyk, J. Skalski, A. Sobiczewski, and S. Ćwiok, Nucl. Phys. **A502**, 591c (1989).
[10] Z. Patyk and A. Sobiczewski, Nucl. Phys. **A533**, 132 (1991).
[11] K. Rutz, M. Bender, T. Bürvenich, T. Schilling, P.-G. Reinhard, J.A. Maruhn, and W. Greiner, Phys. Rev. C **56**, 238 (1997).
[12] S. Ćwiok, J. Dobaczewski, P.-H. Heenen, P. Magierski, and W. Nazarewicz, Nucl. Phys. **A611**, 211 (1996).
[13] W.D. Myers and W.J. Świątecki, Nucl. Phys. **81**, 1 (1966).
[14] S.G. Nilsson, C.F. Tsang, A. Sobiczewski, Z. Szymański, S. Wycech, C. Gustafson, I.L. Lamm, and B. Nilsson, Nucl. Phys. **A131**, 1 (1969).
[15] J. Randrup, S.E. Larsson, P. Möller, A. Sobiczewski, and A. Łukasiak, Phys. Scr. **10A**, 60 (1974).
[16] Z. Patyk, A. Sobiczewski, P. Armbruster, and K.-H. Schmidt, Nucl. Phys. **A491**, 267 (1989).
[17] R. Smolańczuk, J. Skalski, and A. Sobiczewski, Phys. Rev. C **52**, 1871 (1995).
[18] *Table of Isotopes*, 8th ed., edited by R.B. Firestone and V.S. Shirley (Wiley, New York, 1996), Vol. 2.
[19] P. Reiter, T.L. Khoo, C.J. Lister, D. Seweryniak, I. Ahmad, M. Alcorta, M.P. Carpenter, J.A. Cizewski, C.N. Davids, G. Gervais, J.P. Greene, W.F. Henning, R.V.F. Janssens, T. Lauritsen, S. Siem, A.A. Sonzogni, D. Sullivan, J. Uusitalo, I. Wiedenhöver, N. Amzal, P.A. Butler, A.J. Chewter, K.Y. Ding, N. Fotiades, J.D. Fox, P.T. Greenlees, R.-D. Herzberg, G.D. Jones, W. Korten, M. Leino, and K. Vetter, Phys. Rev. Lett. **82**, 509 (1999).
[20] M. Leino, H. Kankaanpää, R.-D. Herzberg, A.J. Chewter, F.P. Hessberger, Y. Le Coz, F. Becker, P.A. Butler, J.F.C. Cocks, O. Dorvaux, K. Eskola, J. Gerl, P.T. Greenlees, K. Helariutta, M. Houry, G.D. Jones, P. Jones, R. Julin, S. Juutinen, H. Kettunen, T.L. Khoo, A. Kleinböhl, W. Korten, P. Kuusiniemi, R. Lucas, M. Muikku, P. Nieminen, R.D. Page, P. Rahkila, P. Reiter, A. Savelius, Ch. Schlegel, Ch. Theisen, W.H. Trzaska, and H.-J. Wollersheim, Eur. Phys. J. A **6**, 63 (1999).
[21] R.-D. Herzberg and M. Leino (private communication).
[22] G. Münzenberg and P. Armbruster, in *Exotic Nuclear Spectroscopy*, edited by W.C. McHarris (Plenum, New York, 1990), p. 181.
[23] G. Münzenberg, S. Hofmann, H. Folger, F.P. Hessberger, J. Keller, K. Poppensieker, B. Quint, W. Reisdorf, K.H. Schmidt, H.J. Schött, P. Armbruster, M.E. Leino, and R. Hingmann, Z. Phys. A **322**, 227 (1985).
[24] I. Muntian, Z. Patyk, and A. Sobiczewski, Acta Phys. Pol. B **30**, 689 (1999); Phys. Rev. C **60**, 041302(R) (1999).
[25] R. Smolańczuk and A. Sobiczewski, in *Proceedings of the XV Nuclear Physics Conference on Low Energy Nuclear Dynamics*, St. Petersburg, Russia, 1995, edited by Yu.Ts. Oganessian, W. von Oertzen, and R. Kalpakchieva (World Scientific, Singapore, 1995), p. 313.
[26] H.J. Krappe, J.R. Nix, and A.J. Sierk, Phys. Rev. C **20**, 992 (1979).
[27] S. Ćwiok, J. Dudek, W. Nazarewicz, J. Skalski, and T. Werner, Comput. Phys. Commun. **46**, 379 (1987).
[28] A. Sobiczewski, Z. Patyk, S. Ćwiok, and P. Rozmej, Nucl. Phys. **A485**, 16 (1988).
[29] P. Möller, J.R. Nix, W.D. Myers, and W.J. Świątecki, At. Data Nucl. Data Tables **59**, 185 (1995).
[30] R.R. Chasman and I. Ahmad, Phys. Lett. B **392**, 255 (1997).
[31] J.F. Berger, L. Bitaud, J. Decharge, M. Girod, and S. Peru-Desenfants, in *Proceedings of the 24th International Workshop on Extremes of Nuclear Stucture*, Hirschegg, Austria, 1996, edited by H. Feldmeier, J. Knoll, and W. Nörenberg (GSI, Darmstadt, 1996), p. 43.
[32] G.A. Lalazissis, M.M. Sharma, P. Ring, and Y.K. Gambhir, Nucl. Phys. **A608**, 202 (1996).
[33] D.R. Inglis, Phys. Rev. **96**, 1059 (1954).
[34] A. Sobiczewski, S. Bjørnholm, and K. Pomorski, Nucl. Phys. **A202**, 274 (1973).
[35] K. Pomorski, B. Nerlo-Pomorska, I. Ragnarsson, R.K. Sheline, and A. Sobiczewski, Nucl. Phys. **A205**, 433 (1973).
[36] I. Ragnarsson, A. Sobiczewski, R.K. Sheline, S.E. Larsson, and B. Nerlo-Pomorska, Nucl. Phys. **A233**, 329 (1974).
[37] I. Hamamoto, Phys. Lett. **56B**, 431 (1975).
[38] K. Pomorski and A. Sobiczewski, Acta Phys. Pol. B **9**, 61 (1978).
[39] J.O. Rasmussen, Phys. Rev. **113**, 1593 (1959); **115**, 1675 (1959).